

## Research Article

## Improving the Semisolid Deformation Behavior and Thixoformability of AZ61 Magnesium Alloy Through Controlling the Strain Induced Melt Activation Process

M. Fatemi Mehrabani<sup>1</sup>, A. Zarei-Hanzaki<sup>1\*</sup> and H.R. Abedi<sup>2\*</sup>

<sup>1</sup> School of Metallurgy and Materials Engineering, College of Engineering, University of Tehran, Tehran, Iran

<sup>2</sup> School of Metallurgy & Materials Engineering, Iran University of Science and Technology (IUST), Tehran, Iran

## ARTICLE INFO

*Article history:*

Received 15 February 2022

Reviewed 27 March 2022

Revised 23 April 2022

Accepted 1 May 2022

*Keywords:*

Magnesium alloys

Semisolid flow behavior

Thixoforming

Thermomechanical processing

Microstructure

## ABSTRACT

The present work deals with the microstructure globularization, coarsening behavior and the correlated kinetics during strain-induced melt activation process of AZ61 magnesium alloy. In this study, the effect of pre-strain, temperature and holding time have been considered, and the evolutions were numerically discussed based on Lifshitz-Slyozov-Wagner (LSW) and Ostwald ripening mechanisms. The treated microstructures (undeformed, globular, non-globular, and coarsened) were then hot compressed at a semisolid temperature range to assess the thixotropic flow behavior of the material. A unique microstructure encompassing fine  $\alpha$ -Mg globules uniformly distributed in the matrix and surrounded by a liquid phase was developed by imposing 45% pre-strain and holding it at 555°C for 8 min. The lowest deformation resistance belonged to the specimens holding globular microstructures, while those with undeformed characteristics possessed the highest flow stress during thixoforming. The semisolid flow response was discussed considering the flow of liquid that incorporates solid particles (FLS); sliding between solid particles (SS), and plastic deformation of solid particles (PDS) mechanisms. The influence of the shape factor (in globular structure) and the grain size (in coarsened structure) on the thixotropic flow behavior of the experimented alloy were also illustrated.

© Shiraz University, Shiraz, Iran, 2022

### 1. Introduction

High specific strength and stiffness, excellent damping capacity, and low density of magnesium alloy make them competent materials for lightweight structures in transportation industries [1-4], however, poor mechanical properties of industrial parts made by low-temperature deformation, restrict their wide applications. Therefore, shear-thinning and thixotropic behavior of partially solidified alloys was the starting

point for semisolid metal (SSM) processing [5]. In this respect, semi-solid processing (SSP) or thixoforming has more prominently studied by many researchers from all over the world due to a lowered forming temperature, increased die life, reduced porosity and solidification shrinkage, and improved mechanical properties. The required stress level for SSP is appreciably lower than that of thermomechanical processing in solid-state, and the mechanical properties of the fabricated component are well higher than those produced through a liquid

\* Corresponding authors

E-mail addresses: [zareih@ut.ac.ir](mailto:zareih@ut.ac.ir) (A. Zarei-Hanzaki), [h Abedi@iust.ac.ir](mailto:h Abedi@iust.ac.ir) (H.R. Abedi)

<https://doi.org/10.22099/IJMF.2022.43073.1218>

metal die-casting [6, 7].

The qualified starting microstructure (feedstock) of thixoforming is non-dendritic, and equiaxed [8] which is prepared through various routes in the liquid state such as: spray forming [9, 10] magneto-hydro-dynamic stirring (MHD), cooling slope (CS) [11], mechanical stirring [12] and in solid-state including strain-induced melt activated (SIMA), and recrystallization and partial melting (RAP) [6, 13]. In comparison with liquid state routes, the solid-state processes are the simplest method with significant commercial advantages [14, 15]. The reduced amount of entrapped liquid and more spherical solid particles, which subsequently result in enhanced thixoformability, make the strain-induced melt activation (SIMA) and recrystallization and partial melting (RAP) the appropriate methods for feedstock preparation of wrought magnesium and aluminum alloy [16-19]. These processes generally consist of initial plastic deformation of work-pieces and subsequent holding isothermally at semisolid temperature to partially re-melt the eutectic phase and stimulate globularization. Different procedures have been employed to impose the required pre-deformation such as upsetting, forging, rolling and extrusion. The penetration of liquid into the recrystallized grain boundaries during soaking leads to the formation of fine equiaxed particles.

From a general point of view, initial microstructure plays an important role not only in semisolid deformation behavior but also in the mechanical properties of thixo-formed components. For instance, Tzimas and Zavaliangos [20] have reported that where the amount of liquid is low at a high-volume fraction of solid ( $>0.6$ ), compressive deformation is highly non-uniform due to the strain localization. They have emphasized the influence of the geometry of solid grains (equiaxed or elongated) in determining the flow response of the thixo-formed material. In the case of magnesium alloys, Wang et al. [21] studied the effect of the initial as-cast microstructure on the semisolid microstructure of AZ91D alloy during the SIMA process. It has been shown that the recrystallization process in the fine-grained as-cast microstructure was

easily motivated and caused evolution from dendrite to fine globular morphology. This was attributed to the higher accumulated stored strain energy due to uniform inner crystal lattice distortion. In addition, the fracture of the narrow secondary dendrite has easily occurred, and finer dendrite could evolve to finer globular grains during partial melting. Despite all the reports [20-24], regarding the preparation of the semisolid slurry and semisolid deformation behavior of magnesium alloys, the effect of starting microstructure (I) on the characteristics of feedstock and (II) on the rheological behavior during thixoforming has been mainly overlooked. In this respect, this work was steered towards studying the influence of SIMA process parameters (pre-strain, temperature and holding time) on the microstructure evolution of slurry with a special emphasis on the kinetic and micro-mechanism of globularization and coarsening. Accordingly, the (I) as-received, (II) globular, (III) non-globular, and (IV) coarsened microstructures were considered as candidates for starting microstructure and the correlated thixo-deformation behaviors were assessed.

## 2. Experimental Procedure

### 2.1. Strain induced melt activation (SIMA) process

AZ61 magnesium alloy in the form of a hot extruded rod by the chemical composition corresponding to the commercial AZ61 grade (Table 1), was used as experimental material. The as-extruded samples were preheated at 350°C for 15 min in an electrical resistance furnace, to remove the deformed state and obtain a homogenized equiaxed microstructure. The specimens (with a diameter of 8 mm and height of 12 mm) were then immediately compressed at 400°C down to 30, 45 and 60% height reduction (height of compressed specimens were 8.4, 6.6, and 4.8 mm, respectively), using a 60-tons hydraulic press with the speed of 18 mm/s. To apply the SIMA process and preparation of the feedstock for thixoforming process, the compressed specimens were

**Table 1.** The chemical composition of AZ61magnesium alloy in wt.%

Mg	Al	Zn	Mn	Si	Cu
Bal.	6.2	0.74	0.22	0.04	$\leq 0.001$

heated up to 540, 555, 570, and 585°C and held at these temperatures for 4, 8, and 12 min. Argon atmosphere was used as the protective atmosphere to prevent oxidization. After the isothermal heat treatment, the samples were just taken out and put into the cooling water immediately.

To achieve the various percentages of liquid and solid phases, the temperatures should be more than solidus (535°C) and less than liquidus (650°C) points. Additionally, in the SIMA process, the percentage of liquid phase should be generally below 50% (595°C in this alloy) [40] to have a combination of flow-ability and good microstructure results which lead to higher mechanical properties. The selected temperatures in this study (540, 555, 575, and 585°C) which meet the requirements of the above items, illustrated the increasing and decreasing trend of globule size and roundness well. It should be mentioned that the temperatures reported in this study, are the actual values measured by a precise thermocouple device.

### 2.2. Microstructure characterization

The SIMA processed specimens were then mechanically polished and chemically etched by an etchant composed of 4.2 g picric acid, 10 ml acetic acid, 10 ml H<sub>2</sub>O, and 70 ml ethanol. The microstructures were then observed through an Olympus PME3 optical microscope. The average grain size and shape factor of solid particles were calculated in each case by using image analyzing software. The grain size and shape factor are defined through Eqs. (1) and (2), respectively [20]:

$$D_{eq} = \frac{\sum_1^N \sqrt{4A/\pi}}{N} \quad (1)$$

$$SF = 1 / \left( \frac{\sum_1^N \frac{P^2}{4\pi A}}{N} \right) \quad (2)$$

where  $A$ , and  $P$ , are the area and perimeter of grains, respectively, and  $N$  is the number of grains. The unity of shape factor drives from full circularity grains and below unity deviates from a circular shape.

### 2.3. Thixoforming process

The specimens holding different initial microstructures were subjected to the thixoforming process through conducting hot compression in the semisolid temperature range. The cylindrical hot compression specimens with a diameter of 12 mm and height of 8 mm were cut from as-received and SIMA processed samples. The tests were carried out at 555°C under the strain rate of 0.01 s<sup>-1</sup> using a Geotech-AI7000 servo-controlled electronic universal testing machine equipped with an electrical resistance furnace. The specimens were coated with a graphite-based lubricant before being put on the anvil to reduce the influence of the friction. At the end of the test, the specimens were rapidly quenched into the water to preserve the deformed microstructure.

## 3. Results and Discussion

### 3.1. Strain induced melt activation process

#### 3.1.1. Effect of pre-strain

The optical micrograph of the AZ61 alloy after annealing of as-received material at 350°C for 15 min (optimum achievable homogenized microstructure to prevent the grain growth) is shown in Fig. 1(a). The microstructures of the annealed specimens which have been hot compressed down to 30, 45, and 60%, and then heated up to 555°C and held for 4 min are illustrated in Fig. 1(b)-1(d). The reason for selecting this soaking time was to analyze the only pre-strain effect on the final microstructure in the SIMA process that can be distinguished at lower holding times (i.e. 4 min). The variation of the roundness and the grain size versus imposed strain is plotted in Fig. 2, which suggests the 45% pre-strain as the optimum condition resulting in the roundest and finest microstructures. The dislocation density of the deformed structure provides a suitable condition for spheroidization of globules through providing high diffusivity paths that increase the kinetics of spheroidization phenomenon [25]. In fact, 60% of the pre-strain leads to providing exceeded activation energy to accelerate the continuous recrystallization, so the recrystallization process has been done earlier in the

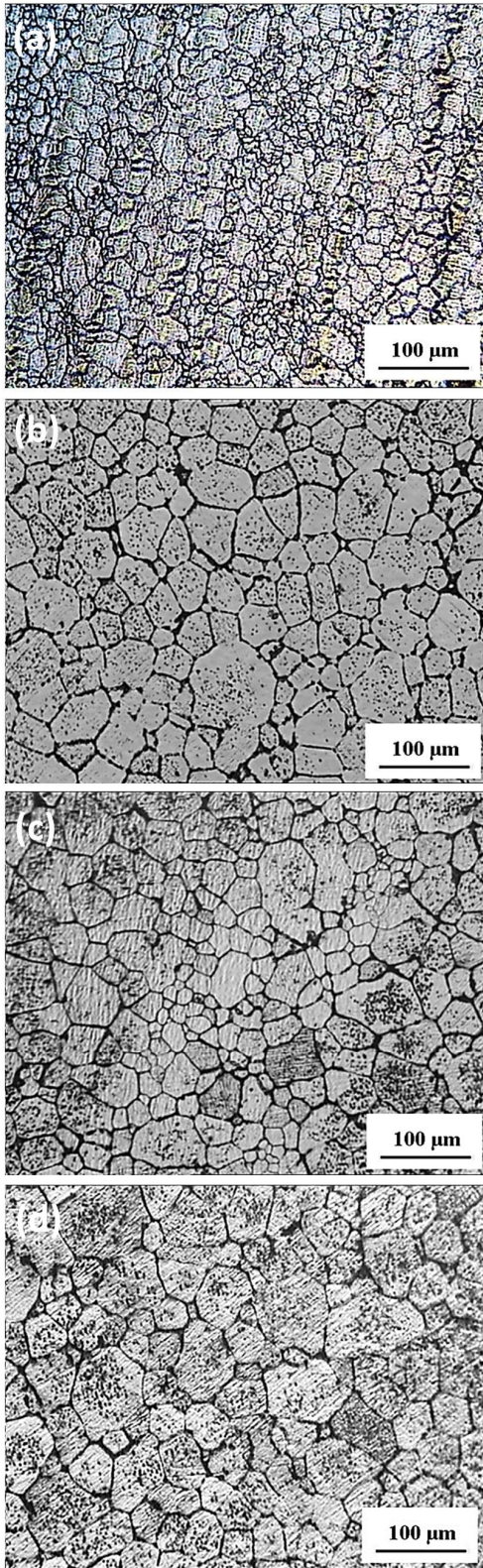


**Fig. 1.** (a) The microstructure of the as-extruded AZ61 alloy which has been annealed at 350°C for 15 min, and microstructures of annealed specimens which have been compressed down to: (b) 30%, (c) 45% and (d) 60% and then heated up to 555°C and soaked for 4 min.

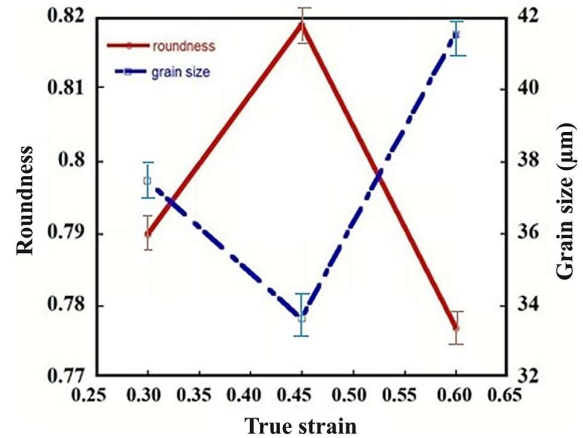


**Fig. 2.** The variations of grain size and roundness with the amount of pre-strain after heat treatment at 555°C for 4 min.

solid-state (before local melting in SIMA process). Therefore, completion of the recrystallization step and initiation of grain growth is associated with a decrease in dislocation density. In this situation, the microstructure will experience growth during subsequent heating in the semisolid range which results in the coalescence of grains. Hence, the merged new grains possess the minimum roundness that can be seen in Fig. 2.

### 3.1.2. Effect of isothermal temperature

The semisolid microstructures which have been obtained through compressive deformation down to 45% followed by heating at 540, 555, 570, and 585°C and holding for 8 min are shown in Fig. 3. As illustrated, the non-uniformity of the grain size and the scarce liquid film around the solid grains are the main characteristics of developed microstructure through isothermal treatment at 540°C (Fig. 3(a)). This is expected to have a negative effect on the thixotropic behavior of semisolid microstructure [26]. In contrast, a globular microstructure containing well-rounded and isolated  $\alpha$ -globules has been formed by increasing the holding temperature to 555°C (Fig. 3(b)). The most important difference between these two figures is the higher amount of liquid film around the solid grains in Fig. 3(b), in contrast to Fig. 3(a), which causes dendritic microstructure in those grain boundaries. In addition, the roundness of grains in Fig. 3(b) is more than Fig. 3(a). By sequences, a significant grain coarsening has occurred in the semisolid

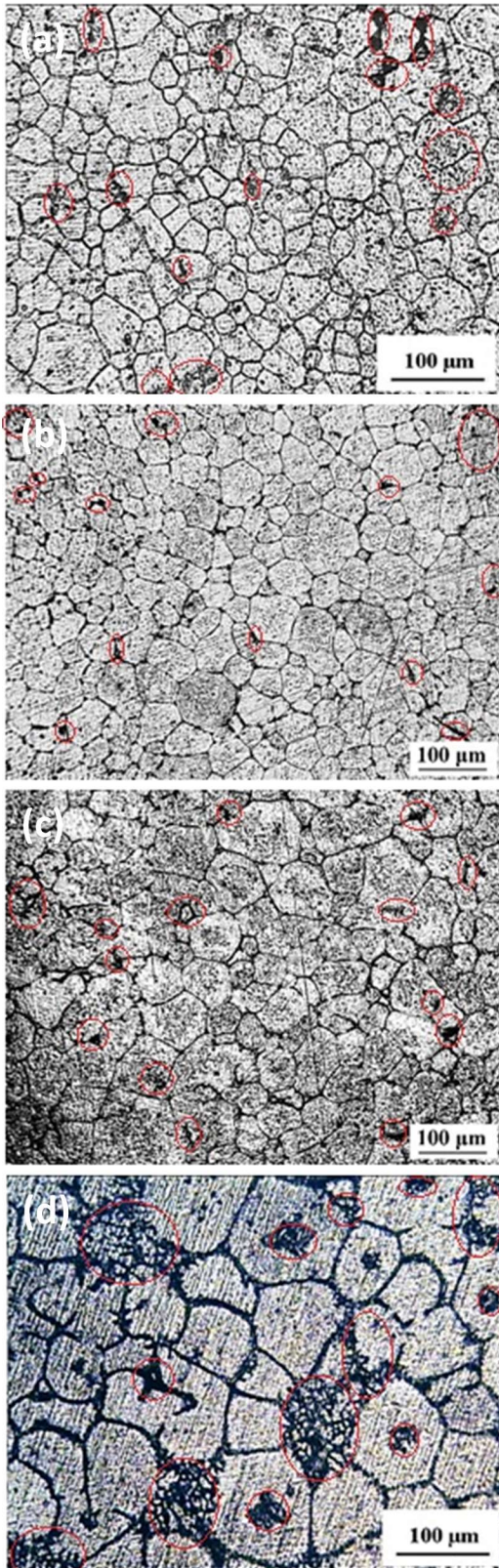


Fig. 3. Microstructure of the specimen compressed down to 45%, heated up to: (a) 540°C, (b) 555°C, (c) 570°C, and (d) 585°C, and soaked for 8 min. Dendritic structure are marked by red lines.

microstructure soaked at 575°C as is illustrated in Fig. 3(c); this is then followed by the formation of high liquid fraction due to partial melting of  $\alpha$ -Mg globule through soaking at 585°C for 8 min (Fig. 3(d)). This can be evidenced by considering the presence of some fine dendritic regions around the globules.

Fig. 4 shows the variations of roundness and globule size of the microstructures compressed down to 45% and soaked at different isothermal temperatures of 540, 555, 575, and 585°C for 8min. The maximum value of roundness ( $\sim 0.82$ ) and minimum value of globule size ( $\sim 42\mu\text{m}$ ) have been obtained at 555°C which may provide the best thixotropic microstructure for subsequent semisolid processing.

More study on the effect of isothermal holding temperature demonstrates that once the penetration of liquid through new recrystallized grain boundaries commences (by the melting of dendrites roots,  $\alpha$ -globules, or incipient melting of  $\beta$ -eutectic phase and other low melting point precipitates), the desired thixotropic microstructure would be available. This eventually leads to a fine and spherical microstructure surrounded by liquid [27]. The capability of the liquid to wet the grain boundaries and penetration depend upon the grain boundary energy which can be categorized into two groups [10]: (I) the solid-solid low-energy grain boundaries ( $\Theta < 20$ ) with low capability for the penetration of the liquid (Fig. 5(a)); these grain boundaries may be obtained during continuous recrystallization or

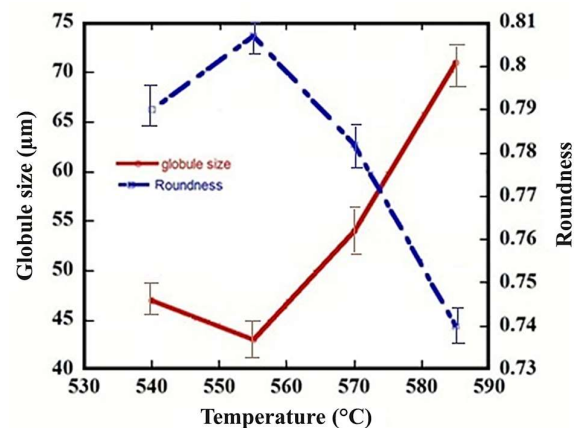
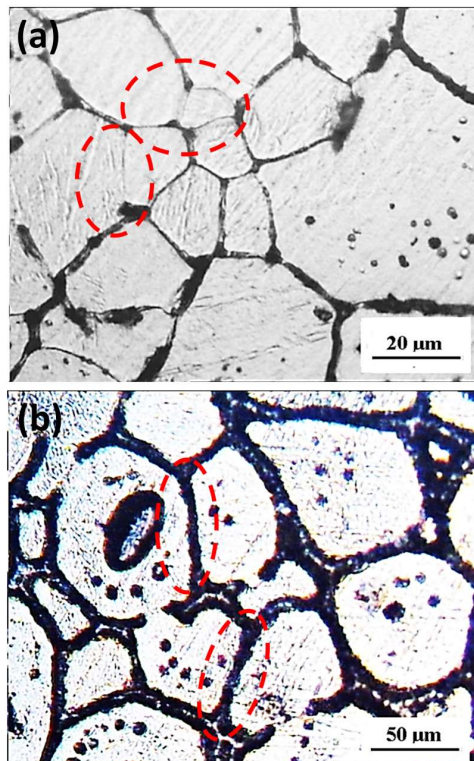
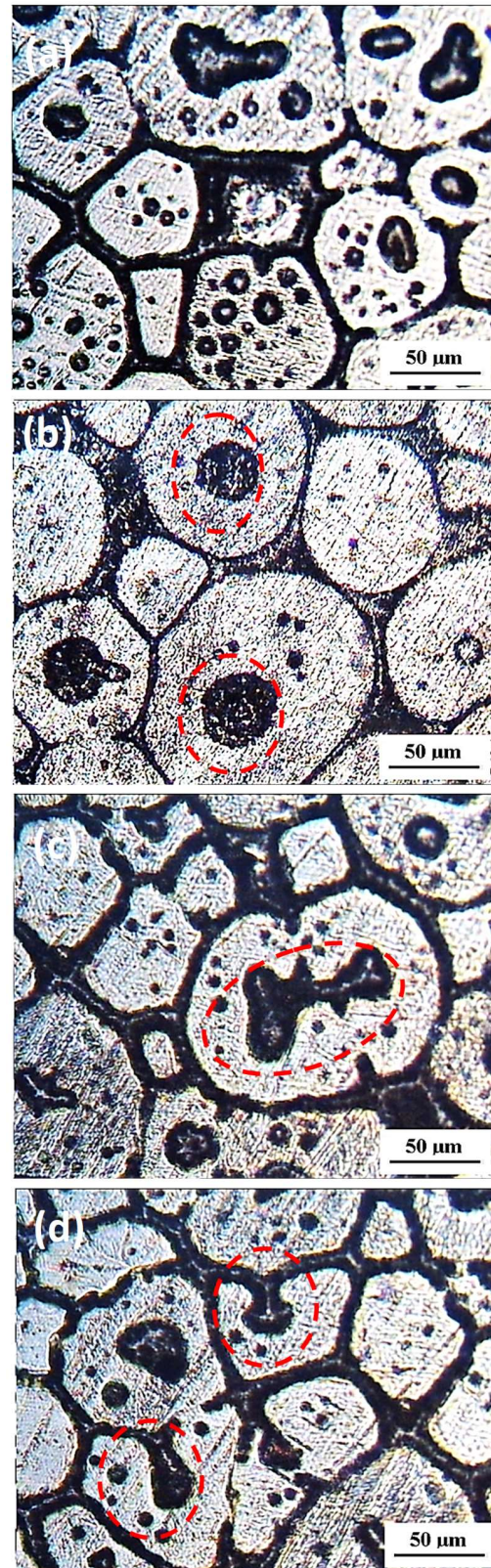


Fig. 4. Variations of the roundness and globule size of the microstructure which has been compressed down to 45% and isothermally held for 8 min at temperatures of 540, 555, 575, and 585°C.

grain boundary migration and grain rotation [10], (II) The high angle grain boundaries, with complete penetration of the liquid, as is shown in Fig. 5(b). Furthermore, some liquid droplets are also visible in all microstructures which have not been situated at the grain boundaries, as shown in Fig. 6. These liquid droplets inside the globules which are ascribed to the chemical segregation and grain coalescence tend to form “entrapped liquid” pools at higher temperatures. This is attributed to the precipitation of  $Mg_{17}Al_{12}$  intermetallic compounds in areas with higher Al and Zn contents, during partial melting [28]. On the other hand, as the result of coalescence, contiguous grains merging into each other lead to the formation of an entrapped pool at their boundaries (Fig. 6(a)). It is of interest to note that intragranular liquid pools inside grains become larger, more spherical, and subtracted in number with increasing holding time, as shown in Fig. 6(b). Owing to coalescence, on the decline of the solid-liquid surface



**Fig. 5.** Typical microstructure of partially re-melted AZ61 magnesium alloy containing (a) low angle (45% pre-strain and heating at 555°C for 4 min soaking), and (b) high angle grain boundaries (45% pre-strain and heating at 585°C for 4 min soaking). These provide the condition for low and complete penetration of liquid.



**Fig. 6.** Liquid pools with different size and morphology formed during partial melting: (a) an irregular shape liquid pool, (b) spheroidized liquid pool, (c) and (d) joining of liquid pools to inter-globular liquid.

area [29] joining of liquid pools to inter-globular liquid phase located at grain boundaries is also probable (Figs. 6(c) and 6(d)). It is considerable to note that, these liquid pools are contributed to micro-porosity formation during the thixoforming process [30].

### 3.1.3. Effect of isothermal holding time

Although the optimum strain for globularity is 45%, regarding its highest roundness and the lowest grain size, the role of holding time cannot be distinguished specifically in the mentioned pre-strain. Therefore, the mechanisms of coarsening during soaking at various times are the most obvious in 60% pre-strain due to enough activation energy for earlier completion of recrystallization and starting the grain growth. The semisolid microstructures of the experimented alloy compressed down to 60% after partial re-melting at 555°C for different holding times of 4, 8, and 12 min are shown in Fig. 7. As can be seen, a partial globular microstructure has been obtained by soaking the specimens for 4 min (Fig. 7(a)). By enhancing atomic diffusion and merging of the particles into each other after holding for 8 min, a well globular microstructure, as well as coarsened grains, have been attained (Fig. 7(b)). Further extending the soaking time leads to more coarsening of the  $\alpha$ -globules (Fig. 7(c)). When isothermal holding times vary from 4 to 12 min, the measured average size of the  $\alpha$ -Mg grains in the semisolid microstructures increases from 49 to 71  $\mu\text{m}$ , respectively.

### 3.1.3. Kinetics and mechanisms of coarsening

For many diffusion-controlled coarsening systems, including solid/liquid mixtures, coarsening kinetics can be described by Eq. (3) with the theory of Lifshitz-Slyozov-Wagner (LSW) as follows:

$$d_t^n - d_0^n = Kt \quad (3)$$

where  $d_t$  and  $d_0$  are the final and initial grain size, respectively,  $t$  is the isothermal holding time,  $K$  is a coarsening rate constant, and  $n$  is the power exponent which is 3 for volume diffusion-controlled coarsening of

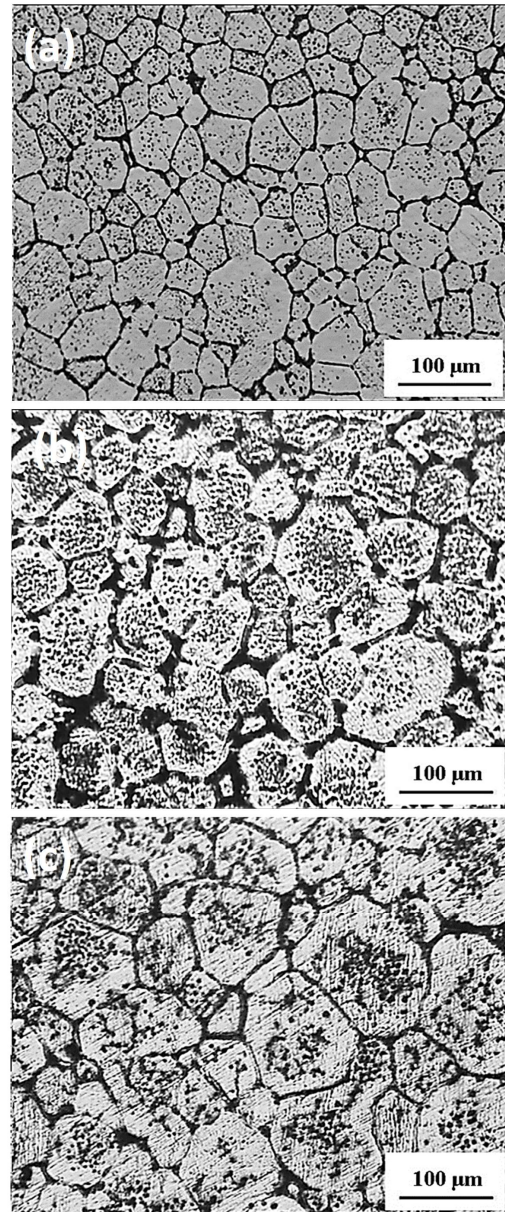
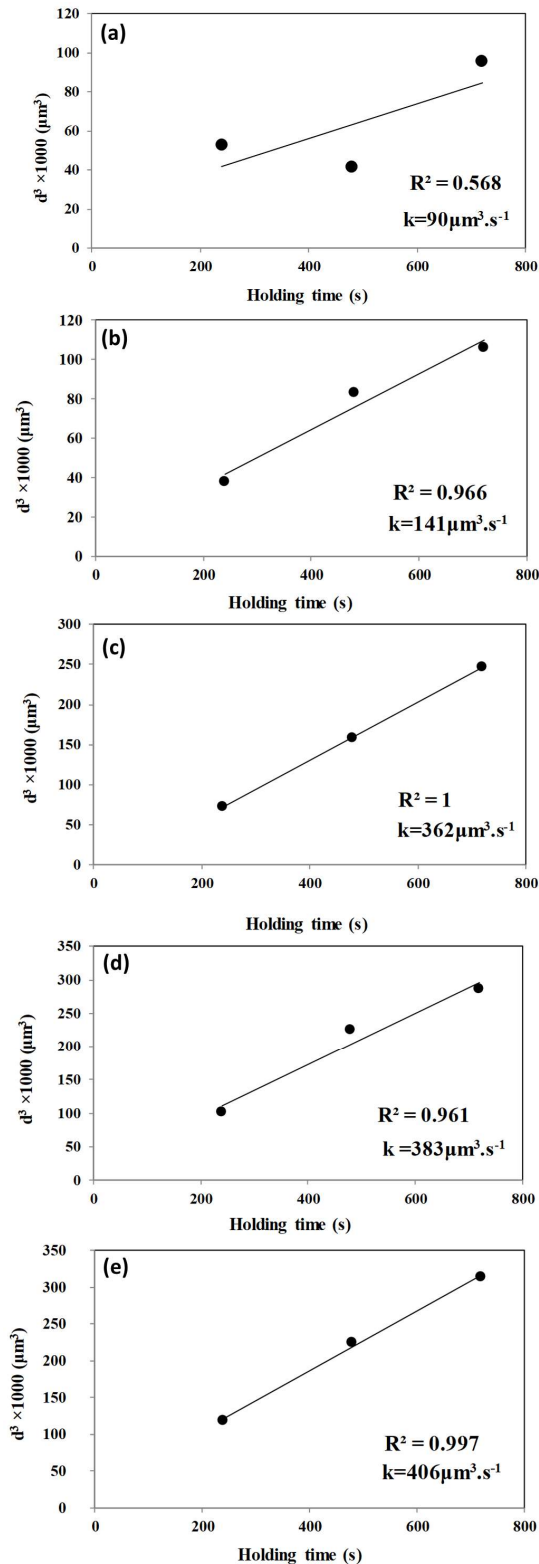


Fig. 7. The microstructures of the alloys compressed down to 60% after heating up to 555°C and holding for: (a) 4 min, (b) 8 min, and (c) 12 min.

metals in the semisolid state reported by many studies [24, 31]. The cubic coarsening rate constant,  $K$ , in the above equation is given experimentally by the gradient of the best fit straight lines as is shown in Fig. 8. It is considerable to note that the deviation from linear coarsening behavior pronounces the contribution of coalescence in grain growth.

During partial re-melting, the grain coarsening is controlled by grain coalescence and Ostwald ripening



**Fig. 8.** Variations of cubed average globules diameter with holding time in compressed microstructure down to 45% at the temperatures of: (a) 540, (b) 555, (c) 570, and (d) 585°C. The results related to the specimen compressed down to 60% and heated at 555°C is also depicted in (e).

mechanism generally [32]. By the inception of liquid formation, coalescence and Ostwald ripening activates synchronously [33]. Due to the formation of thin liquid film at the early stage of partial re-melting, the diffusion process is limited; therefore, the coalescence mechanism mainly controls the grain coarsening [13]. Increasing the holding time ends up with an increment of liquid film and further coarsening by Ostwald ripening takes place [34], where the diameter of bigger grains increases at the expense of smaller ones (the dissolution-precipitation mechanism) [6].

To further examine the kinetics of microstructural evolution in semisolid treatment, the variations of cubed average grain diameter with holding time in the case of specimens compressed down to 45% and heated at temperatures of 540, 555, 570, and 585°C are shown in Fig. 8.  $R^2 = 0.568$  for  $T = 540^\circ\text{C}$  is lower than  $R^2 = 0.966$  for  $T = 555^\circ\text{C}$ ,  $R^2 = 1$  for  $T = 570^\circ\text{C}$  and  $R^2 = 0.961$  for  $T = 585^\circ\text{C}$ , which is attributed to less linearity. Although the points due to Fig. 8(a) seem to be few, from the repeatability of its results in experiments and also in comparison with the linear fitting of other samples, it can be concluded that the linear trend was not observed in Fig. 8(a). This displayed nonlinear behavior indicating that the dominant coarsening mechanism at 540°C is coalescence and does not completely obey the LSW theory. In comparison, kinetics behavior in the rest three plots follows the Ostwald ripening mechanism due to good agreement with the mentioned theory [27]. The relation to the microstructure, which has been compressed down to 60% and heated at 555°C is also given in Fig. 8, which well indicates the higher cubic coarsening rate constant ( $406 \mu\text{m}^3 \text{ s}^{-1}$ ), the higher pre-strain has been imposed.

The coarsening coefficient ( $K$ ) of the microstructure holding different average liquid fraction versus temperature is plotted in Fig. 9. The error bars extracted from the total uncertainty were gained from the repetitions of tests. In addition, the graph followed the same trend in the numerous experiments. As is illustrated, by increasing the temperature (thus increasing liquid fraction) a higher coarsening rate is obtained. This would be rationalized considering the

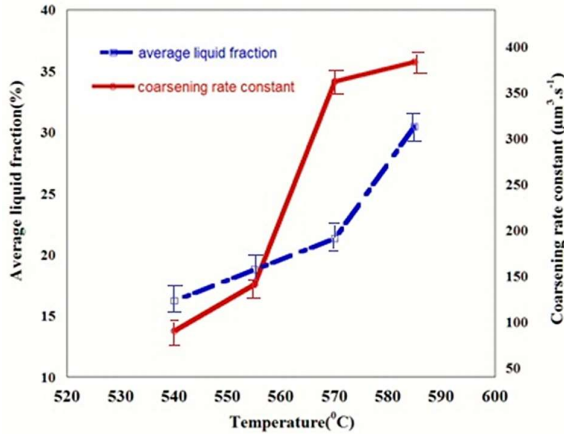


**Fig. 9.** The coarsening rate coefficient of the SIMA processed microstructures and holding different average liquid fraction versus temperature. Specimens were compressed down to 45% and heated at temperatures of 540, 555, 570 and 585°C.

Ostwald ripening as the main coarsening mechanism used at elevated temperatures [27]. However, as Atkinson and Liu [8] have suggested,  $K$  relates not only to the temperature but also to the fraction of liquid. They stated that to estimate the fraction of liquid (not actual values), integrating partial areas under the heating curves of DSC results can be used leading to a much faster diffusion path of liquid than solid. Hence, a continuous liquid path that is present around the globules can accelerate coarsening kinetics. As can be seen, the slope of coarsening coefficient curve then decreases immediately by increasing liquid fraction. This may be rationalized by the thickening of liquid film and accelerated melting of convex edges of merged globules in higher temperature, which finally prohibits the coalescence of grains and leads to making the globules separated.

### 3.2. Thixo-deformation behavior

The prepared feedstocks through the SIMA process have been compressed at 555°C under the strain rate of  $0.01 \text{ s}^{-1}$  to assess the thixo-deformation behavior of the material. The obtained flow stress curves of different starting microstructures are plotted in Fig. 10. As can be seen, the undeformed specimen with non-globular microstructure (with primary phase particles and dendritic or rosette-like morphologies) demonstrates the greatest deformation resistance, while the specimen with

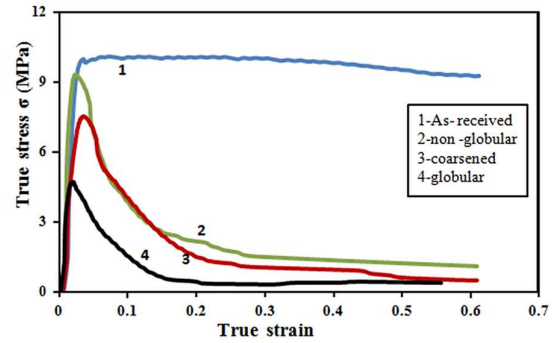


**Fig. 10.** The typical flow curves of the hot compressed specimens at 555°C with different initial microstructures. 1) as received, 2) 30% pre-strain and heated up to 555°C and soaked for 4 min, 3) 60% pre-strain and heated up to 555°C and soaked for 12 min, and 4) 45% pre-strain and heated up to 555°C and soaked for 8 min.

initial globular microstructure indicates the lowest amount in the thixotropic compression process. As mentioned in section 2.1, the as-received samples were preheated at 350°C for 15 min. This preheating removed the deformed state and obtained a homogenized equiaxed microstructure (recrystallized) with coherent and semi-coherent grain boundaries with low values of Gibbs free energy (stable). During the thixoforming process, these stable grain boundaries were resistant to partial melting and sliding; therefore, the level of true stress did not fall. However, for other samples which had previously experienced a SIMA process, the eutectic liquid films around the grains caused high values of Gibbs free energy (unstable) in solid-state. During the thixoforming process, these unstable grain boundaries with low melting points were partially melted beforehand, given that the level of true stress fell and these samples demonstrated lower deformation resistance.

This ideal semisolid microstructure was gained thorough SIMA processing of the specimen considering the pre-strain of 45%, heat treatment temperature of 555°C, and holding time of 8 min (Fig. 3(b)). Fig. 11 displays the appearance of the deformed specimens after thixotropic compression at 555°C under the strain rate of  $0.01 \text{ s}^{-1}$ . As can be observed, the radial and perimeter cracking caused an enormous ruin in the undeformed, non-globular and coarsened globular microstructure of the specimen. To clarify the observed behavior, the deformation mechanism for each condition

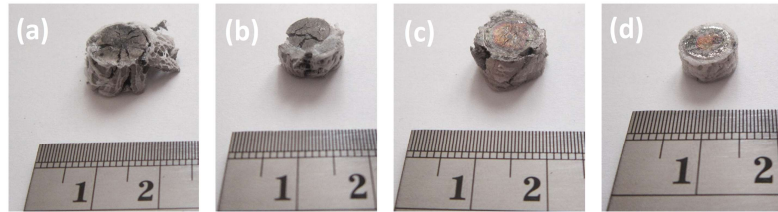


**Fig. 11.** The deformed specimens after hot compression at 555°C with different initial microstructures: (a) as-received, (b) non-globular (30% pre-strain, 555°C, 4 min), (c) coarsened (60% pre-strain, 555°C, 12 min), and (d) globular (45% pre-strain, 555°C, 8 min).

should be characterized. Generally, three deformation mechanisms existed in the whole semisolid forming process: (I) the plastic deformation of solid particles, (II) the sliding between solid particles, and (III) the flow of liquid incorporating solid particles [35, 36]. The mentioned deformation resistance in curve 1 is accordingly derived by the high volume fraction of the solid. The two former mechanisms are active where the solid volume fraction was high and solid particles in the microstructure were in contact with each other. In contrast, where the solid volume fraction was lower, the solid particles were surrounded by liquid phase, and the latter mechanism is considered as the dominant deformation mechanism for the globular microstructures [37]. Therefore, the deformation force was very small and was only required to overcome liquid resistance, which is visible in Fig. 10 (curve 4). Additionally, the growth and coalescence of the globules in the coarsened initial microstructure may lead to their interconnection, which makes the microstructure more resistant and thus requires higher forming pressure (curve 3), compared to the one holding globular initial microstructure. This is attributed to the plastic deformation of solid particles and also sliding between solid particles, as the dominant operative mechanisms [38]. Hence, the higher deformation force is required to overcome the friction generated from the sliding between solid particles, and also to overcome the restriction of the solid particle movement due to the spatial constraint imposed by the surrounding particles [35]. The impact of the shape factor (in globular structure) and the grain size (in coarsened structure) on the thixotropic flow behavior of the experimented alloy is also represented in Fig. 12. In addition, due to a decrease in particle roundness and thus enhanced solid-liquid interaction surface, the increment

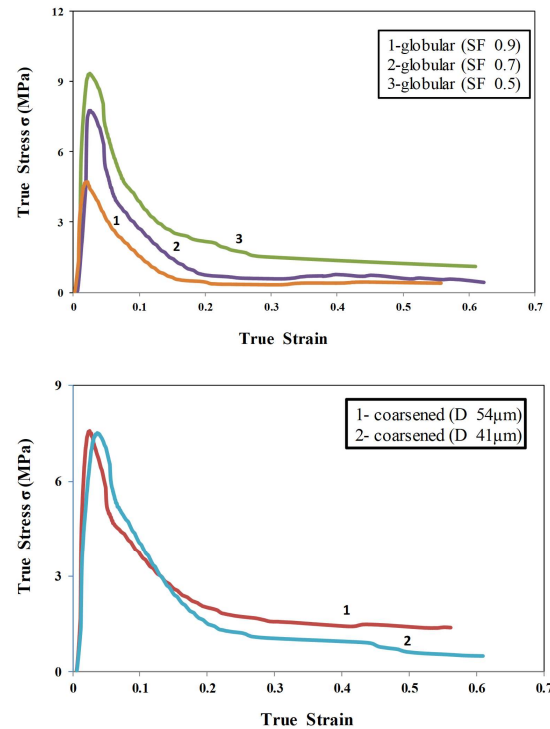


**Fig. 12.** The influence of shape factor (in globular structure with 45% pre-strain, heating at 555°C and soaking time of: (1) 8 min, (2) 12 min, and (3) 4 min), and the grain size (in coarsened structure with 60% pre-strain, heating at 555°C and soaking time of: (1) 12 min, (2) 8 min) on the thixotropic flow behavior of the experimented alloy.

in viscosity of semisolid slurry during coarsening may lead to higher loads to be thixoformed [39]. On the other hand, in the specimens with initial non-globular microstructures containing large volume fractions of interconnected solid particles, larger stress is required which implies the plastic deformation rather than sliding between solid particle mechanisms. As previously mentioned, the liquid phase fails to lubricate the movements of the solid phase [19], therefore, the solid grains are disabled to move smoothly to accommodate the imposed strain.

Fig. 13 shows a flowchart summarizing the details,

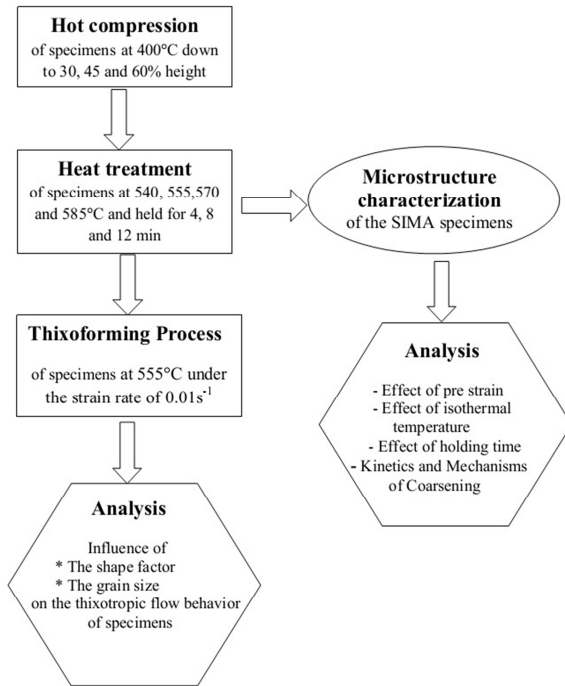


**Fig. 13.** Flowchart on the details, selected experimental parameters, characterized properties and evaluated mechanisms.

selected experimental parameters, characterized properties and evaluated mechanisms.

#### 4. Conclusion

Undeformed, globular, non-globular, and coarsened microstructures of as-extruded AZ61 magnesium alloy were treated through a strain-induced melt activated process, and the evolved microstructures were studied in detail to improve the thixotropic flow behavior of the material. The following sequels were extracted:

1. The most appropriate microstructure for the subsequent thixoforming process (by the globules size of 43  $\mu\text{m}$  and the shape factor of 0.81) was achieved through the strain-induced melt activated process considering the pre-strain of 45%, heating temperature of 555°C, and a soaking time of 8 min.
2. The liquid phase completely penetrated through the high angle grain boundaries with greater energy than the solid/liquid interface and in contrast, the liquid was disabled to completely penetrate and wet the low energy solid-solid grain boundaries.
3. Increasing the isothermal soaking time almost

caused a linear increment of cubed average grain diameter which suggested that the coarsening kinetics followed the principles of the Lifshitz-Slyozov-Wagner (LSW) model.

4. The coarsening rate constant ( $K$ ) value was connected to the temperature and liquid fraction. The continuous liquid path around the globules provided a fast diffusion path and accelerated coarsening kinetics. However, liquid film thickening and accelerated melting of convex edges of merged globules at higher temperatures prohibited further coalescence of the grains.
5. The specimens with undeformed and globular starting microstructures exhibited the greatest and the lowest flow resistance during the thixoforming process, respectively. The former was attributed to the plastic deformation and the sliding of solid particles and the latter to the flow of liquid incorporating solid particles.

#### Conflict of Interests

The authors declare that they have no known competing financial interests or personal relationships that could have appeared to influence the work reported in this paper.

#### 5. References

- [1] M. Kohzu, F. Yoshida, H. Somekawa, Fracture mechanism and forming limit in deep-drawing of magnesium alloy AZ31, *Materials Transactions*, 42(7) (2001) 1273-1276.
- [2] S.H. Hsiang, J.L. Kuo, An investigation on the hot extrusion process of magnesium alloy sheet, *Journal of Materials Processing Technology*, 140(1-3) (2003) 6-12.
- [3] Y. Nishikawa, K. Matsumura, A. Takara, Development of the outer cases for television set with magnesium alloy, *Materia Japan*, 39(3) (2000) 278-280.
- [4] S. Kleiner, O. Beffort, A. Wahlen, P.J. Uggowitzer, Microstructure and mechanical properties of squeeze cast and semi-solid cast MgAl alloys, *Journal of Light Metals*, 2(4) (2002) 277-280.
- [5] S. Kleiner, O. Beffort, P. J. Uggowitzer, Microstructure evolution during reheating of an extruded Mg-Al-Zn

- alloy into the semisolid state, *Scripta Materialia*, 51(5) (2004) 405-410.
- [6] Z. Zhao, Q. Chen, H. Chao, S. Huang, Microstructural evolution and tensile mechanical properties of thixoforged ZK60-Y magnesium alloys produced by two different routes, *Materials & Design*, 31(4) (2010) 1906-1916.
- [7] P. Kapranos, P.J. Ward, H.V. Atkinson, D.H. Kirkwood, Near net shaping by semi-solid metal processing, *Materials & Design*, 21(4) (2000) 387-394.
- [8] D. Liu, H.V. Atkinson, H. Jones, MTDATA thermodynamic prediction of suitability of alloys for thixoforming, Proceeding S2P 8<sup>th</sup> International Conference, 2004.
- [9] E. Tzimas, A. Zavaliangos, A comparative characterization of near-equiaxed microstructures as produced by spray casting, magneto-hydrodynamic casting and the stress induced, melt activated process, *Materials Science and Engineering: A*, 289(1-2) (2000) 217-227.
- [10] E. Tzimas, A. Zavaliangos, Evolution of near-equiaxed microstructure in the semisolid state, *Materials Science and Engineering: A*, 289(1-2) (2000) 228-240.
- [11] Y. Birol, A357 thixoforming feedstock produced by cooling slope casting, *Journal of Materials Processing Technology*, 186(1-3) (2007) 94-101.
- [12] R. Haghayeghi, E.J. Zoqui, A. Halvae, M. Emamy, An investigation on semi-solid Al-7Si-0.3Mg alloy produced by mechanical stirring, *Journal of Materials Processing Technology*, 169(3) (2005) 382-387.
- [13] S. Luo, Q. Chen, Z. Zhao, Effects of processing parameters on the microstructure of ECAE-formed AZ91D magnesium alloy in the semi-solid state, *Journal of Alloys and Compounds*, 477(1-2) (2009) 602-607.
- [14] T.J. Chen, G.X. Lu, Y. Ma, Y.D. Li, Y. Hao, Microstructural evolution during partial remelting of equal channel angular pressed ZW21 magnesium alloy, *Journal of Alloys and Compounds*, 486(1-2) (2009) 124-135.
- [15] A. Khosravani, H. Aashuri, P. Davami, A. Narimannezhad, R. Hadian, Liquid segregation behavior of semi-solid AZ91 alloy during back extrusion test, *Journal of Alloys and Compounds*, 477(1-2) (2009) 822-827.
- [16] B. Nami, S.G. Shabestari, S.M. Miresmaeili, H. Razavi, Sh. Mirdamadi, The effect of rare earth elements on the kinetics of the isothermal coarsening of the globular solid phase in semisolid AZ91 alloy produced via SIMA process, *Journal of Alloys and Compounds*, 489(2) (2010) 570-575.
- [17] M.R. Rokni, A. Zarei-Hanzaki, H.R. Abedi, N. Haghdad, Microstructure evolution and mechanical properties of backward thixoextruded 7075 aluminum alloy, *Materials & Design*, 36 (2012) 557-563.
- [18] T.J. Chen, Y. Hao, J. Sun, Microstructural evolution of previously deformed ZA27 alloy during partial remelting, *Materials Science and Engineering: A*, 337(1-2) (2002) 73-81.
- [19] S.B. Hassas-Irani, A. Zarei-Hanzaki, B. Bazaz, A.A. Roostaei, Microstructure evolution and semi-solid deformation behavior of an A356 aluminum alloy processed by strain induced melt activated method, *Materials & Design*, 46 (2013) 579-587.
- [20] E. Tzimas, A. Zavaliangos, Mechanical behavior of alloys with equiaxed microstructure in the semi-solid state at high solid content, *Acta Materialia*, 47(2) (1999) 517-528.
- [21] J.G. Wang, H.Q. Lin, Y.Q. Li, Q.C. Jiang, Effect of initial as-cast microstructure on semisolid microstructure of AZ91D alloy during the strain-induced melt activation process, *Journal of Alloys and Compounds*, 457(1-2) (2008) 251-258.
- [22] F. Czerwinski, A. Zielinska-Lipiec, The melting behaviour of extruded Mg-8%Al-2%Zn alloy, *Acta Materialia*, 51(11) (2003) 3319-3332.
- [23] F. Czerwinski, Near-liquidus molding of Mg-Al and Mg-Al-Zn alloys, *Acta Materialia*, 53(7) (2005) 1973-1984.
- [24] Z. Zhao, Q. Chen, C. Hu, D. Shu. Microstructure and mechanical properties of SPD-processed an as-cast AZ91D+ Y magnesium alloy by equal channel angular extrusion and multi-axial forging, *Materials & Design*, 30(10) (2009) 4557-4561.
- [25] K. Ding, L. Hengcheng, J. Qiumin, T. Yun, Effect of hot extrusion on mechanical properties and microstructure of near eutectic Al-12.0% Si-0.2% Mg alloy, *Materials Science and Engineering: A*, 527(26) (2010) 6887-6892.
- [26] J.F. Jiang, L.I.N. Xin, W.A.N.G. Ying, J.J. Qu, S.J. Luo, Microstructural evolution of AZ61 magnesium alloy pre-deformed by ECAE during semisolid isothermal treatment, *Transactions of Nonferrous Metals Society of China*, 22(3) (2012) 555-563.
- [27] N. Haghdad, A. Zarei-Hanzaki, S. Heshmati-Manesh, H.R. Abedi, S.B. Hassas-Irani, The semisolid microstructural evolution of a severely deformed A356 aluminum alloy, *Materials & Design*, 49 (2013) 878-887.
- [28] F. Czerwinski, Size evolution of the unmelted phase during injection molding of semisolid magnesium alloys, *Scripta Materialia*, 48(4) (2003) 327-331.
- [29] Q. Chen, J. Lin, D. Shu, C. Hu, Z. Zhao, F. Kang, S. Huang, B. Yuan, Microstructure development, mechanical properties and formability of Mg-Zn-Y-Zr

- magnesium alloy, *Materials Science and Engineering: A*, 554 (2012) 129-141.
- [30] D.G. Eskin, V.I. Savran, L. Katgerman, Effects of melt temperature and casting speed on the structure and defect formation during direct-chill casting of an Al-Cu alloy, *Metallurgical and Materials Transactions A*, 36(7) (2005) 1965-1976.
- [31] S. Ashouri, M. Nili-Ahmadabadi, M. Moradi, M. Iranpour, Semi-solid microstructure evolution during reheating of aluminum A356 alloy deformed severely by ECAP, *Journal of Alloys and Compounds*, 466(1-2) (2008) 67-72.
- [32] D. Fan, S.P. Chen, L.Q. Chen, P.W. Voorhees, Phase-field simulation of 2-D Ostwald ripening in the high volume fraction regime, *Acta Materialia*, 50(8) (2002)1895-1907.
- [33] F. Czerwinski, On the generation of thixotropic structures during melting of Mg-9%Al-1%Zn alloy, *Acta Materialia*, 50(12) (2002) 3267-3283.
- [34] Z. Fan, Semisolid metal processing, *International Materials Reviews*, 47(2) (2002) 49-85.
- [35] C.P. Chen, C.Y. Tsao, Semi-solid deformation of non-dendritic structures Phenomenological behavior, *Acta Materialia*, 45(5) (1997) 1955-1968.
- [36] H. Yan, B. Zhou, Thixotropic deformation behavior of semi-solid AZ61 magnesium alloy during compression process, *Materials Science and Engineering: B*, 132(1-2) (2006) 179-182.
- [37] H.R. Abedi, A. Zarei-Hanzaki, S.M. Fatemi-Varzaneh, A.A. Roostaei, The semi-solid tensile deformation behavior of wrought AZ31 magnesium alloy, *Materials & Design*, 31(9) (2010) 4386-4391.
- [38] E.R.D. Freitas, E.G. Ferracini Júnior, V.P. Piffer, M. Ferrante, Microstructure, material flow and tensile properties of A356 alloy thixoformed parts, *Materials Research*, 7(4) (2004) 595-603.
- [39] E.J. Zoqui, M.H. Robert, Structural modifications in rheocast Al-Cu alloys by heat treatment and implications on mechanical properties, *Journal of Materials Processing Technology*, 78(1-3) (1998) 198-203.
- [40] M. Easton, D. StJohn, Grain refinement of aluminum alloys: Part I. The nucleant and solute paradigms-a review of the literature, *Metallurgical and Materials Transactions A*, 30(6) (1999), 1613-1623.